

A mutation in autosomal dominant myotonia congenita affects pore properties of the muscle chloride channel

(*CLCN1*/permeation/skeletal muscle/electrophysiology)

CHRISTOPH FAHLKE, CAROL L. BECK, AND ALFRED L. GEORGE, JR.*

Departments of Medicine and Pharmacology, Vanderbilt University School of Medicine, Nashville, TN 37232

Contributed by Michael V. L. Bennett, Albert Einstein College of Medicine, Bronx, NY, January 8, 1997 (received for review September 26, 1996)

ABSTRACT Autosomal dominant myotonia congenita is an inherited disorder of skeletal muscle caused by mutations in a voltage-gated Cl⁻ channel gene (*CLCN1*, 7q35). Here, we report that a mutation predicting the substitution of Gly 230 by glutamic acid (G230E) between segments D3 and D4 dramatically alters the pore properties of a recombinant human muscle Cl⁻ channel (hClC-1) expressed in a mammalian cell line (tsA201). The G230E mutation causes substantial changes in anion and cation selectivity as well as a fundamental change in rectification of the current–voltage relationship. Whereas wild-type channels are characterized by pronounced inward rectification and a Cl > thiocyanate > Br > NO₃ > I > CH₃SO₃ selectivity, G230E exhibits outward rectification at positive potentials and a thiocyanate > NO₃ > I > Br > Cl > CH₃SO₃ selectivity. Furthermore, the cation-to-anion permeability ratio of the mutant is much greater than that of the wild-type channel. Voltage-dependent blocks by intracellular and extracellular iodide help to distinguish two distinct ion binding sites within the hClC-1 conduction pathway. Both binding sites are preserved in the mutant but have decreased affinities for iodide. These findings suggest that Gly 230 is critical for normal ion conductance in hClC-1 and that this residue resides within the channel pore.

Voltage-gated chloride channels belonging to the ClC family are involved in a variety of cellular functions (1), but their gating and ion permeation properties are incompletely understood. Recently, important insights into the structure–function relationships of this ion channel family have been gained from investigations of disease-producing genetic mutations in the skeletal muscle ClC-1 (2, 3).

In both autosomal dominant myotonia congenita (Thomsen disease) and recessive generalized myotonia, mutations in the gene encoding the major skeletal muscle Cl⁻ channel (*CLCN1*, 7q35) (4–7) result in reduced sarcolemmal Cl⁻ conductance (g_{Cl}). This abnormal membrane property causes myofiber hyperexcitability (8), repetitive firing of muscle action potentials, and clinical myotonia characterized by muscle stiffness upon sudden forceful movement (9). One recently described functional disturbance exhibited by a variety of muscle ClC-1 mutations responsible for dominant myotonia congenita caused a shift in the voltage dependence of channel activation to more positive membrane potentials and resulted in a reduced open probability at the resting membrane potential of skeletal muscle (10, 11). Another *CLCN1* mutation found in a patient with recessive generalized myotonia caused distinct abnormalities in channel gating (3).

The first reported *CLCN1* mutation discovered in Thomsen disease causes the substitution of a highly conserved glycine residue by glutamic acid located between putative transmembrane segments D3 and D4 in human ClC-1 (5). A previous study examining the functional characteristics of this mutation in a recombinant human muscle ClC-1 (hClC-1) using the *Xenopus* oocyte expression system concluded that the mutation renders the channel nonfunctional when expressed alone but that coexpression with the wild-type (WT) allele partially rescues function (2). The results of this study were used to infer that hClC-1 is a multimeric ion channel and suggested a possible mechanism to explain the dominant-negative effect of Thomsen disease mutations.

Because of potential experimental limitations with the *Xenopus* oocyte expression system for the study of Cl⁻ channels, we sought to evaluate the functional characteristics of the G230E mutation in a mammalian cell line. Our results demonstrate a dramatic change in the ion selectivity of the mutant channel, suggesting a, to our knowledge, novel molecular mechanism of myotonia congenita and a possible role of Gly 230 in hClC-1 pore function.

MATERIALS AND METHODS

Construction and Expression of G230E. Site-directed mutagenesis was performed as described (3). Two independent recombinant mutant clones were subcloned back into the full length hClC-1 cDNA in both pSP64T and pRc/CMV vectors for expression studies. Transient transfections of tsA201 cells were performed using 10–15 μg of plasmid DNA using a calcium phosphate precipitation method as described (12). Stably transfected HEK-293 cells were used for some experiments examining WT hClC-1 (3). No differences were observed between results obtained in tsA201 and HEK-293 cells. To identify cells with a high probability of expressing recombinant ion channels, cells were cotransfected with a plasmid encoding the CD8 antigen and incubated 5 min before use with polystyrene microbeads precoated with anti-CD8 antibody (Dynabeads M-450 CD 8, Dynal, Great Neck, NY) (13). Only cells decorated with microbeads were used for electrophysiological recordings. Cells were typically examined 2 days after transient transfection.

Electrophysiology. Standard whole cell recordings (14) were performed and analyzed as described (15). For the description of the time course of current deactivation, a sum of two exponentials and a time-independent value [$I(t) = a_1 \exp(-t/\tau_1) + a_2 \exp(-t/\tau_2) + d$] were fit to data recorded during a series of hyperpolarizing voltage steps from a holding potential of 0 mV. Fractional amplitudes of current deactivation components were calculated by dividing the individual records by

The publication costs of this article were defrayed in part by page charge payment. This article must therefore be hereby marked “advertisement” in accordance with 18 U.S.C. §1734 solely to indicate this fact.

Copyright © 1997 by THE NATIONAL ACADEMY OF SCIENCES OF THE USA
0027-8424/97/942729-6\$2.00/0
PNAS is available online at <http://www.pnas.org>.

Abbreviations: hClC, human muscle ClC; WT, wild-type; G230E, the substitution of Gly 230 by glutamic acid; K_D, dissociation constant; g_{Cl} , chloride conductance.

*To whom reprint requests should be addressed. e-mail: al.george@mcmail.vanderbilt.edu.

the peak current amplitude (I_{\max}) determined after a long (>500 ms) prepulse to 55 mV: $A_1 = a_1/I_{\max}$, $A_2 = a_2/I_{\max}$, $C = d/I_{\max}$. To obtain the voltage dependence of activation, the instantaneous current amplitude determined 200 μ s after a voltage step to -135 mV was measured after prepulses to different voltages (V) and then divided by its maximum value. The normalized data were then plotted vs. the preceding potential. This plot yields the voltage dependence of the relative open probability, P_{open} , at the end of the prepulse. The steady state activation curve was obtained by using 1.4-s prepulses. Steady state activation curves obtained in this manner were fitted with a single Boltzmann term and a voltage-independent value: $I(V) = \text{Amp} \cdot \{1 + \exp[(V - V_{0.5})/k_V]\}^{-1} + \text{constant}$. Cells were clamped to 0 mV for at least 15 s between test sweeps.

Unless otherwise noted, the compositions of the solutions were as follows: standard external solution (in mM): NaCl (140), KCl (4), CaCl_2 (2), MgCl_2 (1), and Hepes (5, pH 7.4); and standard internal solution (in mM): CsCl (130), MgCl_2 (2), EGTA (5), Hepes (10, pH 7.4). In experiments examining the effects of external iodide, measurements were performed first in standard external solution, and then NaI was added to a final concentration of 30 mM. For experiments examining the effect of intracellular iodide, cells were perfused with a solution containing (in mM) CsI (40), CsCl (90), MgCl_2 (2), EGTA (5), and Hepes (10, pH 7.4) and were bathed in standard external solution. Agar bridges were used to connect the bath solution to the amplifier to avoid junction potentials. Offset potentials were measured at the end of experiments and were used to correct results. Contribution of leak current was negligible under these conditions (15). All data are shown as means \pm SEM.

Determination of Ion Permeability Ratios. Current-voltage curves for hClC-1 do not obey the Goldman-Hodgkin-Katz equation, and therefore ion permeation is not expected to follow the assumptions of the Goldman-Hodgkin-Katz theory (16). In this study, we have applied this relationship simply as an operational definition of the permeability ratio.

To determine cation/anion permeability ratios, current reversal potentials (E_{rev}) were measured in the whole cell configuration with solutions of different ionic compositions and were used to solve for P_X/P_{Cl} in the following equation:

$$E_{\text{rev}} = \frac{RT}{F} \ln \frac{P_X[X^+]_o + P_{\text{Cl}}[\text{Cl}^-]_i}{P_X[X^+]_i + P_{\text{Cl}}[\text{Cl}^-]_o}$$

where subscript *i* and *o* indicate intracellular and extracellular concentrations, respectively, and *X* is a cation. Divalent cations were considered to be nonpermeant for this calculation.

In one set of experiments, cells were perfused internally with (in mM) XCl (130), MgCl_2 (2), EGTA (5), and Hepes (10, pH 7.4) and were bathed in an extracellular solution containing (in mM) XCl (144), CaCl_2 (1), MgCl_2 (1), and Hepes (5, pH 7.4) where *X* was either Na^+ or K^+ . After an equilibration period of 2–3 min, the external solution was changed to (in mM) XCl (219), CaCl_2 (1), MgCl_2 (1), and Hepes (5, pH 7.4), and the reversal potential was measured every 30 s. Maximum values of E_{rev} were used for the calculation of P_X/P_{Cl} . In a second approach, cells were perfused internally with (in mM): choline chloride (134), EGTA (5), and Hepes (10, pH 7.4) and bathed in a solution containing (in mM) XCl (150), CaCl_2 (1), and Hepes (5, pH 7.4). Reversal potentials were measured after a 2–3 min equilibration period after establishing the whole cell patch clamp and were used to calculate P_X/P_{Cl} . In these

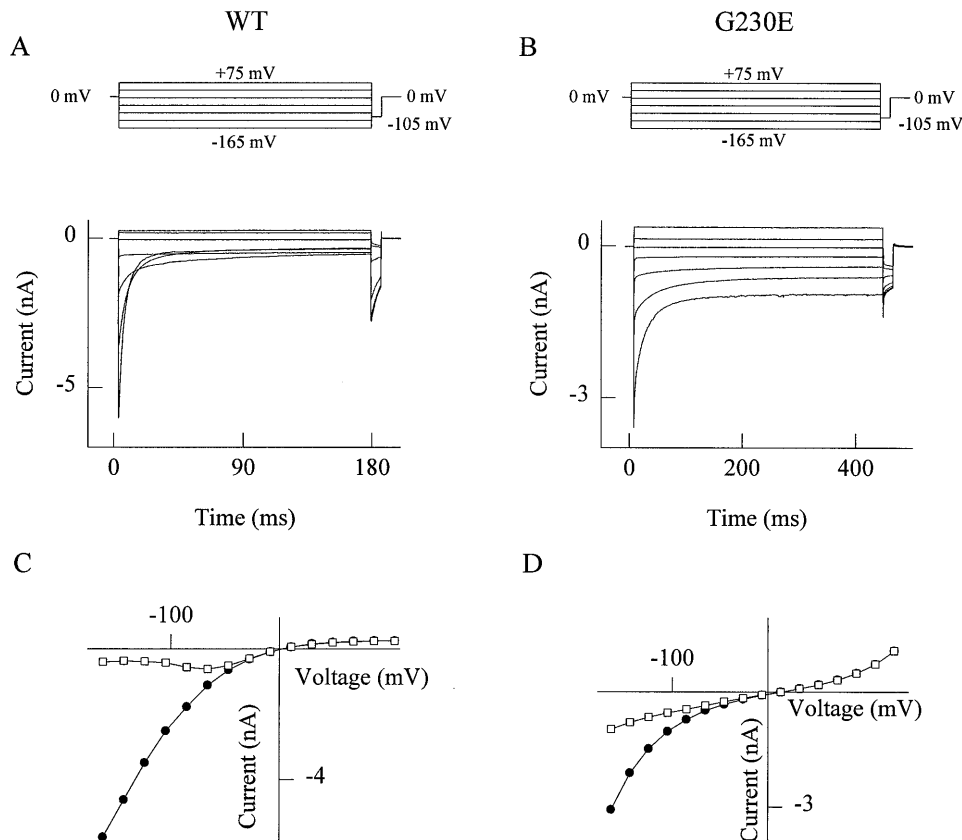


FIG. 1. General properties of WT and G230E hClC-1 channels. (A) Currents recorded from a cell expressing WT hClC-1 channels at voltage steps between -165 mV and +75 mV in 40-mV increments. (B) Currents recorded from a cell transiently transfected with G230E hClC-1. (C and D) Current-voltage relationships for WT (C) and G230E (D). Current amplitudes were measured immediately after the voltage step (filled circles) or at the end of the test pulse (open squares) from recordings shown in A and B.

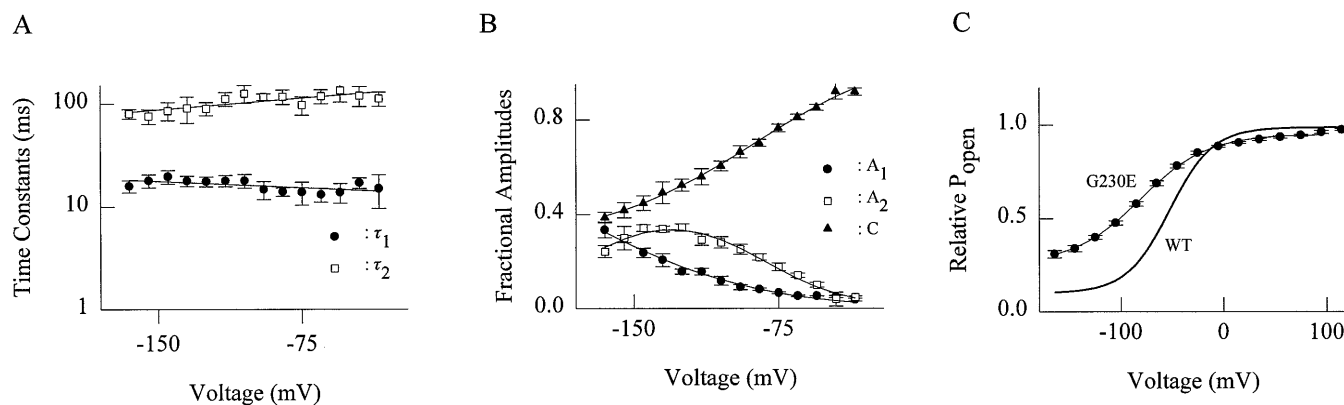


FIG. 2. Gating properties in G230E hClC-1 channels. (A) Voltage dependence of the time constants of deactivation. Closed circles, τ_1 ; open squares, τ_2 (mean \pm SEM from four different cells). (B) Voltage dependence of the fractional current amplitudes. Closed circles, A_1 , open squares, A_2 , and closed triangles, A_3 . (C) Voltage dependence of activation for G230E (mean \pm SEM, $n = 6$) and WT hClC-1 (WT data are taken from figure 6 of reference 15).

experiments, choline and divalent cations were considered nonpermeant.

Similarly, anion permeability ratios were evaluated by measuring reversal potentials in cells perfused internally with (in mM): NaCl (130), MgCl₂ (2), EGTA (5), and Hepes (10, pH 7.4) and bathed in an external solution containing (in mM): NaY (140), KCl (4), CaCl₂ (2), and Hepes (5, pH 7.4) where Y denotes various anions. Reversal potentials were measured within 2–3 minutes after establishing the whole cell patch clamp and were used to calculate P_Y/P_{Cl} ratios by solving:

$$E_{rev} = \frac{RT}{F} \ln \frac{P_{Na}[Na^+]_o + P_K[K^+]_o + P_{Cl}[Cl^-]_i}{P_{Na}[Na^+]_i + P_{Cl}[Cl^-]_o + P_Y[Y^-]_o}$$

Lower limit values obtained experimentally for P_{Na}/P_{Cl} and P_K/P_{Cl} were used in these calculations.

RESULTS

Functional Characterization of G230E. We expressed the G230E mutation in both oocytes and in transiently transfected tsA201 cells. In oocytes, the mutant expressed poorly, and its functional attributes could not be adequately distinguished from endogenous oocyte currents. By contrast, G230E expressed well in tsA201 cells (mean peak current amplitude, 2.3 ± 0.2 nA 48 h after transfection at a test potential of -125 mV; $n = 13$ consecutive cells) although the level of channel expression (as judged by peak current amplitude) was less than that observed for the WT channel transiently expressed in the same cells (mean peak current amplitude, 11.3 ± 2.0 nA at a test potential of -125 mV 24 h after transfection; $n = 8$ consecutive cells). Currents greater than 0.5 nA never were observed in untransfected cells. Currents exhibited by cells expressing the G230E mutant increased instantaneously upon hyperpolarization, followed by a voltage-dependent deactivation, which was slower and less complete than for WT hClC-1 channels (Fig. 1). Upon depolarizing voltage steps, the recorded currents were nearly time-independent for both mutant and WT (Fig. 1A and B). In contrast to the pronounced inward rectification of WT hClC-1 (Fig. 1C), the instantaneous current–voltage relationship of G230E displayed inward rectification in the negative voltage range and outward rectification at positive potentials (Fig. 1D). Also unlike WT hClC-1, G230E currents reversed at a positive potential (5.7 ± 0.7 mV; $n = 11$) in the presence of standard solutions. Similar observations were made for two independent G230E recombinants.

In standard solutions, the gating properties of G230E hClC-1 channels exhibited many characteristics similar to WT channels. Deactivation (as well as activation) of WT and

G230E currents have been well described by a sum of two exponentials and a time-independent value (3, 15). Time constants have minimal voltage dependence (Fig. 2A) whereas fractional current amplitudes (Fig. 2B), representing the percentage of channels in one of three different kinetic states (fast deactivating, slow deactivating, nondeactivating), display marked voltage dependence (15). Compared with the WT channel, deactivation time constants measured at -145 mV were increased ≈ 3 -fold (WT: $\tau_1 = 6.1 \pm 0.3$ ms, $\tau_2 = 35.1 \pm 2.8$ ms, $n = 4$; G230E: $\tau_1 = 19.8 \pm 3.0$ ms, $\tau_2 = 86.0 \pm 17.1$ ms, $n = 4$), and the voltage dependencies of the fractional current amplitudes appeared to be shifted in the hyperpolarizing direction.

Fig. 2C shows activation curves for both WT and G230E. Unlike other dominant myotonia mutations that cause shifts in the voltage dependence of activation toward more positive potentials (10, 11), G230E shifted activation to a more negative voltage range. The voltage dependence of G230E activation was well fit with a single Boltzmann function having an inflection point at -77.7 ± 1.6 mV ($n = 6$) (WT, -52.4 ± 0.8 mV), a slope factor of 27.7 ± 1.1 mV ($n = 6$) (WT, 20.2 ± 0.9 mV), and a constant value of 0.35 ± 0.03 ($n = 6$) (WT, 0.11 ± 0.02). These data indicate that, near the resting membrane potential of skeletal muscle (-85 mV), the relative open probability of G230E is actually greater than WT hClC-1 (Fig. 2C). Therefore, alterations of gating properties in G230E cannot explain the reduction of macroscopic sarcolemmal g_{Cl} associated with this dominantly inherited mutation.

G230E Mutation Altered Ion Selectivity of hClC-1. The change in rectification of the instantaneous current amplitude raised the question whether the G230E mutation affects other pore properties of hClC-1. The positive reversal potential observed for G230E currents under standard ionic conditions suggests an increased cation-to-anion permeability ratio with $Na > Cs$ permeability. To test cation selectivity of G230E and WT hClC-1 channels, reversal potentials in cells expressing

Table 1. Permeability ratios for various anions measured for WT and G230E

Anion	WT		G230E	
	E_{rev}	P_Y/P_{Cl}	E_{rev}	P_Y/P_{Cl}
Br ⁻	9.8 ± 2.5	0.6 ± 0.1	-12.2 ± 2.4	1.7 ± 0.2
I ⁻	21.3 ± 0.7	0.3 ± 0.1	-21.7 ± 0.7	2.6 ± 0.1
SCN ⁻	-0.8 ± 1.2	0.9 ± 0.1	-45.5 ± 3.1	7.2 ± 1.8
NO ₃ ⁻	12.1 ± 1.3	0.5 ± 0.1	-25.5 ± 1.2	3.0 ± 0.2
CH ₃ SO ₃ ⁻	32.8 ± 0.6	0.2 ± 0.1	23.6 ± 4.1	0.2 ± 0.1

$n = 4$ for each experiment. E_{rev} , current reversal potential in millivolts; P_Y/P_{Cl} , permeability ratio for anion Y; SCN⁻, thiocyanate.

mutant or WT hClC-1 channels were measured in solutions with different anion and cation compositions, and these data were used for the calculation of permeability ratios with the Goldman-Hodgkin-Katz equation (16). The cation-to-anion permeability ratio in G230E was found to be substantially increased using two different experimental approaches. In the first experiment, in which we modified the external cation concentration, $P_{\text{Na}}/P_{\text{Cl}}$ and $P_{\text{K}}/P_{\text{Cl}}$ were found to be 0.50 ± 0.05 ($n = 9$) and 0.53 ± 0.05 ($n = 6$), respectively. By contrast, WT hClC-1 exhibited a much stronger anion over cation selectivity ($P_{\text{Na}}/P_{\text{Cl}} = 0.07 \pm 0.01$; $n = 8$). In the other experimental approach, in which cells were perfused with a presumed impermeant cation (choline), $P_{\text{Na}}/P_{\text{Cl}}$ and $P_{\text{K}}/P_{\text{Cl}}$ were determined to be 0.28 ± 0.05 ($n = 12$) and 0.28 ± 0.07 ($n = 6$), respectively ($P_{\text{Na}}/P_{\text{Cl}}$ for WT = 0.00; $n = 8$). The differences in the permeability ratios determined for G230E by the two methods were most likely caused by experimental limitations. In the first experimental approach, hypertonic cell shrinkage may have contributed to increased intracellular ionic concentration, and therefore the calculated permeability ratios may be overestimated. By contrast, the second method would underestimate the permeability ratios if the permeability of choline was greater than 0. The range of values determined here thus represents upper and lower limits. Therefore, by two different experimental approaches, the mutant exhibited a substantial increase in relative cation-to-anion permeability compared with the WT channel.

The G230E mutation also affected the anion selectivity sequence of the hClC-1 pore. Several anions were tested for their ability to permeate G230E and WT hClC-1 channels

(Table 1). Whereas WT hClC-1 channels passed anions with a permeability sequence of $\text{Cl} > \text{thiocyanate} > \text{Br} > \text{NO}_3 > \text{I} > \text{CH}_3\text{SO}_3$, G230E exhibited a markedly altered selectivity sequence with $\text{thiocyanate} > \text{NO}_3 > \text{I} > \text{Br} > \text{Cl} > \text{CH}_3\text{SO}_3$.

G230E Mutation Altered Iodide Block of hClC-1. These prominent changes in ion selectivity prompted us to further investigate the ion conduction pathway in WT and mutant hClC-1 by functionally probing the pore with another halide ion, iodide. Both extracellular and intracellular iodide block Cl^- current through the WT channel, but iodide exerts distinct effects on gating depending on which side of the membrane it is applied. These different effects of iodide on gating properties allow two separate ion binding sites within the pore to be identified.

Extracellular iodide causes a voltage-dependent reduction in the instantaneous current of WT hClC-1 (Fig. 3*A* and *C*). The extent of iodide block measured as the ratio of blocked to unblocked instantaneous current is greatest at positive potentials for a given iodide concentration (0.33 ± 0.05 and 0.05 ± 0.02 for test potentials of -145 mV and 55 mV, respectively, in 30 mM NaI). To determine if the binding site for extracellular iodide is located within the hClC-1 pore, we examined the effect of lowering the intracellular Cl^- concentration on the apparent dissociation constant (K_D) for iodide block. By fitting the unblocked current component to $K_D/(K_D + [\text{I}^-])$, we determined the K_D at a single test potential (75 mV) for two different intracellular Cl^- concentrations. For internal Cl^- concentrations of 134 mM and 14 mM, the apparent K_D values were 2.4 mM and 1.3 mM, respectively. This apparent interaction of internal Cl^- ions with external iodide is consistent

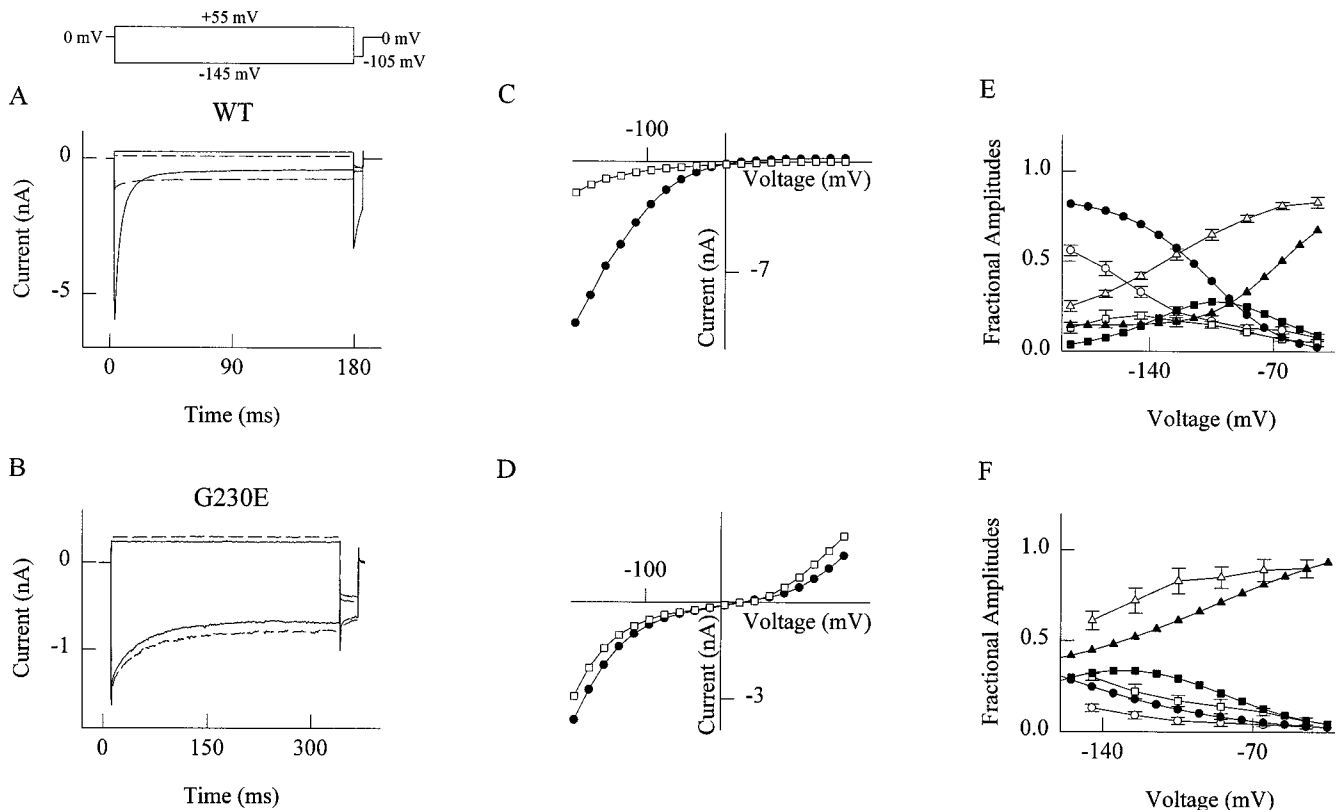


FIG. 3. Effect of extracellular iodide on WT and G230E. (*A*) Current responses to voltage steps from a holding potential of 0 mV to -145 mV and 55 mV recorded from a cell stably expressing WT hClC-1 channels before (solid lines) and after (dashed line) addition of 30 mM NaI to the extracellular solution. (*B*) Current responses to voltage steps from a holding potential of 0 mV to -145 mV and 55 mV recorded from a cell stably expressing G230E channels before (solid lines) and after (dashed line) addition of 30 mM NaI to the extracellular solution. (*C* and *D*) Voltage dependence of the instantaneous current amplitude for WT (*C*) and G230E (*D*) before (closed circles) and after (open squares) addition of 30 mM NaI to the extracellular solution. Test potentials were preceded by a 500 -ms prepulse to 50 mV. (*E* and *F*) Voltage dependence of fractional current amplitudes, obtained as described in Fig. 2 for WT (*E*) and G230E (*F*). Results in the presence (open symbols) or absence (filled symbols) of extracellular 30 mM iodide. Fractional current amplitudes are: circle, A_1 , square, A_2 , and triangle, C. Data shown are mean \pm SEM ($n = 4$).

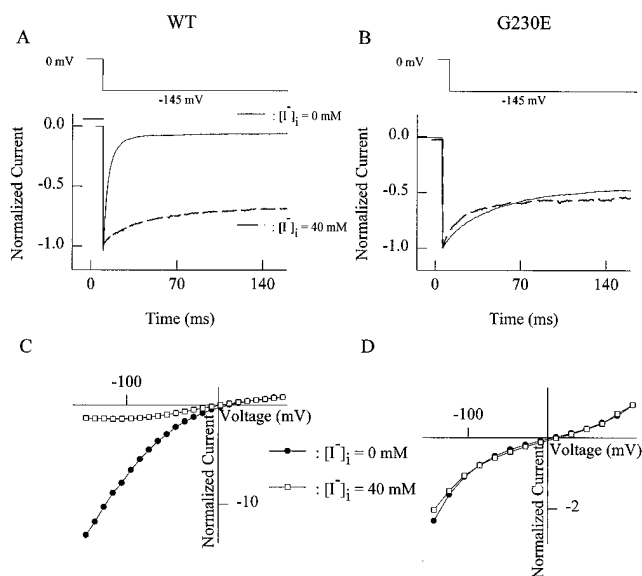


FIG. 4. Effect of intracellular iodide on WT and G230E. (A) Current responses in a cell expressing WT hCIC-1 to a voltage step from 0 mV to -145 mV in standard extracellular solution. Current recordings from one cell perfused with standard intracellular solution (solid line) are superimposed by recordings from another cell with an intracellular solution containing (in mM): CsI (40), CsCl (90), MgCl₂ (2), EGTA (5), and Hepes (10), pH 7.4 (dashed line). Currents are normalized to the peak current amplitude. (B) Current recordings from a cell transfected with G230E using an identical protocol as described for A. (C and D) Voltage dependence of the instantaneous current amplitude for WT (C) and G230E (D) recorded in the absence (filled symbols) and presence (open symbols) of 40 mM intracellular CsI. Data are from experiments shown in A and B and are normalized to current values obtained at 75 mV.

with competitive binding of iodide to a site within the ion conduction pathway (17).

In WT hCIC-1, extracellular iodide also caused a shift in the voltage dependence of the fractional current amplitudes toward more negative potentials (Fig. 3E) without affecting the deactivation time constants (unpublished work). In 30 mM extracellular iodide, a greater fraction of channels either deactivate with slow time constants or do not deactivate, and this causes the apparent "slowing" of the deactivation process and the increased current amplitude at the end of the voltage step (Fig. 3A). In contrast to the WT channel, external iodide has little effect on the instantaneous current conducted by cells expressing G230E (Fig. 3B). In fact, current conducted by G230E channels at positive potentials is slightly increased after addition of 30 mM NaI (Fig. 3D). Although external iodide fails to block G230E channels, it does exert small effects on gating properties that are qualitatively similar to those observed for WT channels. Deactivation time constants are unchanged by external iodide (data not shown); however, the voltage dependencies of the fractional current amplitudes are affected. As observed for the WT channel, the voltage dependence of the nondeactivating current component appears shifted toward more negative potentials in the presence of external iodide (Fig. 3F). We interpret these findings as an indication that this ion binding site within the pore of G230E is functionally intact but has a lower affinity for iodide.

Intracellular iodide also blocks the instantaneous current amplitude in cells expressing WT hCIC-1 and exerts significant effects on channel gating (Fig. 4A and C). Internal perfusion of cells expressing WT hCIC-1 with an iodide-containing solution causes slowing of deactivation and a large increase in both fast (τ_1) and slow (τ_2) deactivation time constants (at -125 mV, $[I^-]_i = 0$ mM: $\tau_1 = 9.1 \pm 1.2$ ms and $\tau_2 = 65.5 \pm 12$, $n = 7$; for $[I^-]_i = 40$ mM: $\tau_1 = 57.6 \pm 10.2$ ms and $\tau_2 =$

391.6 ± 42.3 ms, $n = 4$). We have shown recently that the channel gate is affected by changes in internal Cl⁻ concentration and internal pH, suggesting a direct interaction between the ion pore and the gate from the cytoplasmic side of the membrane (15). The increase of deactivation time constants caused by internal iodide further suggests an ion binding site within the pore (unpublished work).

By contrast to the WT channel, internal iodide does not exert a blocking action on G230E (Fig. 4B and D), but deactivation is changed. When measured with a test pulse to -125 mV, deactivation time constants are decreased in the presence of 40 mM internal iodide ($\tau_1 = 11.9 \pm 1.5$ ms and $\tau_2 = 50.5 \pm 7.6$ ms; $n = 4$) compared with standard internal solution ($[I^-]_i = 0$ mM: $\tau_1 = 17.7 \pm 2.0$ ms and $\tau_2 = 90.1 \pm 12.9$ ms; $n = 4$; $P < 0.05$ for the differences between the presence and absence of iodide). We interpret these findings as evidence that the ion binding site within the pore that is accessible to internal iodide remains functionally intact in G230E but exhibits a lower affinity for iodide.

DISCUSSION

A Novel Mechanism for Myotonia Congenita. The functional characterization of Cl⁻ channel mutations found in dominant or recessive myotonia congenita have illustrated a variety of mechanisms to explain the reduction of sarcolemmal g_{Cl} at the resting potential of the muscle fiber. In addition to nonsense or frameshift mutations, several missense mutations have been shown to produce nonfunctional channels in *Xenopus* oocytes, and these findings have been interpreted as a loss of function (2, 10, 18). All myotonia mutations shown so far to produce functional Cl⁻ channels reduce macroscopic g_{Cl} by affecting gating properties of hCIC-1. Abnormal gating may occur because of an apparent disabling of the channel's voltage sensor (3) or by shifting the midpoint of voltage-dependent activation to more positive potentials by an unclear mechanism (10, 11). By contrast, alterations in the gating of G230E cannot account for a decrease in muscle g_{Cl} associated with this dominantly inherited mutation.

We have characterized the G230E mutation by heterologous expression in a mammalian cell line and have revealed a dramatic change in fundamental pore properties of the channel. Specifically, the mutation causes a change in the relative permeability to cations and an altered selectivity sequence for permeant anions. The magnitude of expressed current in G230E-expressing cells is lower than that of cells transfected with WT. Because of its low single channel conductance (<1 pS) (19), we cannot distinguish low current amplitudes caused by intrinsic channel dysfunction from that caused by decreased cell surface expression of the protein.

We can speculate that the increased Na⁺ permeability of G230E channels may be an additional pathophysiological factor in the genesis of myotonia. As shown for hereditary diseases of the muscle sodium channel, an increased Na⁺ influx at the resting potential is sufficient to cause myotonic repetitive firing in muscle fibers (20, 21). The increased cation permeability exhibited by G230E may be an additional factor in the disease pathogenesis. Our results further suggest that an inability to record Cl⁻ currents in *Xenopus* oocytes injected with mutant hCIC-1 RNA may not be sufficient proof of nonfunction. The observations made with G230E indicate that reevaluation of other "nonfunctional" hCIC-1 alleles in mammalian cells will be worthwhile and potentially informative.

Implications for the Structure and Function of the hCIC-1 Ion Pore. The different effects of intracellular and extracellular iodide on WT and G230E hCIC-1 currents point to the existence of at least two different anion binding sites within the conduction pathway. Occupation of the inner site by iodide in WT hCIC-1 impaired the interaction of the intracellular "gate" with the pore leading to slowed deactivation. By contrast,

binding of iodide to the external site had no effect on the deactivation time constants but did cause changes in the voltage dependence of the fractional current amplitudes. The preservation of these gating effects of iodide observed in G230E suggests that both binding sites were intact. Our current understanding of ion selectivity in hCIC-1 (unpublished work) is that ions that bind more tightly within the pore (e.g., iodide) block the channel and are less permeant than ions that bind less tightly (e.g., Cl^-). The inability of iodide to block G230E corresponds to the $\text{I} > \text{Cl}$ permeability and is consistent with reduced affinity of an intra-pore ion binding site for iodide.

At present, a structural interpretation of our results is impaired by the existence of two different proposed transmembrane topologies for CIC channels (22, 23), predicting the location of Gly 230 to be either at the outer (23) or inner (22) membrane surface. The effects of this mutation on two different ion binding sites accessible to iodide from either inside or outside the cell argue in favor of a close proximity of Gly 230 to the ion pore. The observed changes in ion selectivity caused by the G230E mutations might arise from a direct structural change in the hCIC-1 pore or be the result of an allosteric effect on permeation. All of our observations would be explained well if Gly 230 was in fact a residue within the pore-forming region of the channel, but we cannot provide definitive evidence to support this idea.

Introduction of a negatively charged glutamate residue in or near the pore lumen could serve as a binding site for positively charged ions as in cation selective channels (24, 25). In G230E, electrostatic repulsion of negatively charged ions by the substituted glutamic acid residue would decrease the anion flux and weaken the interaction of blocking anions with sites in the ion conduction pathway.

Other regions of the channel may also contribute to ion selectivity and general permeation properties. Studies of *Torpedo* CIC-0 have revealed a lysine residue (K519) that may contribute to ion binding. Charge reversal mutations at this position result in altered relative conductance of the channel in the presence of Br^- or NO_3^- , reduced iodide block, and changes in rectification of the current-voltage curve (23). Lys 519 is located at the cytoplasmic end of putative transmembrane segment D12 and is conserved in many CIC channels including hCIC-1. The effect of mutating this residue in hCIC-1 is not currently known. Together, these experiments on CIC-0 and our present findings suggest that the CIC ion pore may be formed by multiple channel domains, including portions of segments D3 and D12.

We thank Louis DeFelice for critical review of the manuscript. This work was supported by grants from the Muscular Dystrophy Association (A.L.G.) and the Lucille P. Markey Charitable Trust. Ch. F. is

supported by the Deutsche Forschungsgemeinschaft (Fa301/1-1). C.L.B. is a recipient of the Louis and Emma Benzak Neuromuscular Disease Research Fellowship from the Muscular Dystrophy Association. A.L.G. is a Lucille P. Markey Scholar.

- Jentsch, T. J. (1994) *Curr. Top. Membr. Transp.* **42**, 35–57.
- Steinmeyer, K., Lorenz, C., Pusch, M., Koch, M. C. & Jentsch, T. J. (1994) *EMBO J.* **13**, 737–743.
- Fahlke, Ch., Rüdell, R., Mitrovic, N., Zhou, M. & George, A. L., Jr. (1995) *Neuron* **15**, 463–472.
- Koch, M. C., Steinmeyer, K., Lorenz, C., Ricker, K., Wolf, F., Otto, M., Zoll, B., Lehmann-Horn, F., Grzeschik, K. H. & Jentsch, T. J. (1992) *Science* **257**, 797–800.
- George, A. L., Crackower, M. A., Abdalla, J. A., Hudson, A. J. & Ebers, G. C. (1993) *Nature Genet.* **3**, 305–310.
- George, A. L., Jr., Sloan-Brown, K., Fenichel, G. M., Mitchell, G. A., Spiegel, R. & Pascuzzi, R. M. (1994) *Hum. Mol. Genet.* **3**, 2071–2072.
- Meyer-Kleine, C., Steinmeyer, K., Ricker, K., Jentsch, T. J. & Koch, M. C. (1995) *Am. J. Hum. Genet.* **57**, 1325–1334.
- Adrian, R. H. & Bryant, S. H. (1974) *J. Physiol. (London)* **240**, 505–515.
- Thomsen, J. (1876) *Arch. Psychiatr. Nervenkrankh.* **6**, 702–718.
- Pusch, M., Steinmeyer, K., Koch, M. C. & Jentsch, T. J. (1995) *Neuron* **15**, 1455–1463.
- Beck, C. L., Fahlke, Ch. & George, A. L., Jr. (1996) *Proc. Natl. Acad. Sci. USA* **93**, 11248–11252.
- Fahlke, Ch., Knittle, T. J., Gurnett, C. A., Campbell, K. P. & George, A. L., Jr. (1997) *J. Gen. Physiol.* **109**, 93–104.
- Jurman, M. E., Boland, L. M., Liu, Y. & Yellen, G. (1994) *BioTechniques* **17**, 876–881.
- Hamill, O. P., Marty, A., Neher, E., Sakmann, B. & Sigworth, F. J. (1981) *Pflügers Arch.* **391**, 85–100.
- Fahlke, Ch., Rosenbohm, A., Mitrovic, N., George, A. L., Jr. & Rüdell, R. (1996) *Biophys. J.* **71**, 695–706.
- Hille, B. (1992) *Ionic Channels of Excitable Membranes* (Sinauer, Sunderland, MA).
- Armstrong, C. M. (1971) *J. Gen. Physiol.* **58**, 413–437.
- Lorenz, C., Meyer-Kleine, C., Steinmeyer, K., Koch, M. C. & Jentsch, T. J. (1994) *Hum. Mol. Genet.* **3**, 941–946.
- Pusch, M., Steinmeyer, K. & Jentsch, T. J. (1994) *Biophys. J.* **66**, 149–152.
- Lehmann-Horn, F., Kuther, G., Ricker, K., Grafe, P., Ballanyi, K. & Rüdell, R. (1987) *Muscle Nerve* **10**, 363–374.
- Cannon, S. C., Brown, R. H., Jr. & Corey, D. P. (1993) *Biophys. J.* **65**, 270–288.
- Middleton, R. E., Pheasant, D. J. & Miller, C. (1994) *Biochemistry* **33**, 13189–13198.
- Pusch, M., Ludewig, U., Rehfeldt, A. & Jentsch, T. J. (1995) *Nature (London)* **373**, 527–530.
- Heinemann, S. H., Terlau, H., Stühmer, W., Imoto, K. & Numa, S. (1992) *Nature (London)* **356**, 441–443.
- Yang, J., Ellinor, P. T., Sather, W. A., Zhang, J. & Tsien, R. W. (1993) *Nature (London)* **366**, 158–161.